

PAPER

Optical analysis, optical limiting and electrical properties of novel PbI_2/PVA polymeric nanocomposite films for electronic optoelectronic applications

To cite this article: N Sabry *et al* 2019 *Mater. Res. Express* **6** 115339

View the [article online](#) for updates and enhancements.



IOP | ebooksTM

Bringing you innovative digital publishing with leading voices to create your essential collection of books in STEM research.

Start exploring the collection - download the first chapter of every title for free.

Materials Research Express



PAPER

Optical analysis, optical limiting and electrical properties of novel PbI_2/PVA polymeric nanocomposite films for electronic optoelectronic applications

RECEIVED
21 September 2019

REVISED
3 October 2019

ACCEPTED FOR PUBLICATION
8 October 2019

PUBLISHED
18 October 2019

N Sabry¹, M I Mohammed^{1,4}  and I S Yahia^{2,3} 

¹ Nanoscience Laboratory for Environmental and Biomedical Applications (NLEBA), Metallurgical Lab.1., Department of Physics, Faculty of Education, Ain Shams University, Roxy, 11757 Cairo, Egypt

² Research Center for Advanced Materials Science (RCAMS), King Khalid University, Abha 61413, P O Box 9004, Saudi Arabia

³ Advanced Functional Materials & Optoelectronic Laboratory (AFMOL), Department of Physics, Faculty of Science, King Khalid University, PO Box 9004, Abha, Saudi Arabia

⁴ Author to whom any correspondence should be addressed.

E-mail: mrfismail@yahoo.com

Keywords: PVA/ PbI_2 , nanocomposite films, optical/bandgap analysis, AC electrical conductivity, dielectric properties, optoelectronic devices

Abstract

This paper studied the influence of changing the lead iodide (PbI_2), concentration in the PVA matrix through the structural, optical and electric measurements. Nanocomposite films have been defined by X-ray diffraction and FT-IR spectrometer which reveal the interaction between PVA and PbI_2 . The interplanar distance, particle size, and the average inter-crystalline separation were calculated. The optical properties of PbI_2/PVA composites have been examined. PVA optical band gap was reduced from 5 to 3.49 in indirect transition and from 5.48 to 4.88 indirect transition to cause an increase in optical conductivity. Dielectric constant, ϵ_1 and dielectric loss, ϵ_2 and electrical conductivity, σ is increased with increasing PbI_2 concentrations. So, the electrical conductivity σ can be controlled by the PbI_2 doping percentage. PbI_2/PVA showed laser power attenuation for both He-Ne and solid-state green laser beams. The results indicate that the nanocomposites are highly recommended in optoelectronic, radiation detection and many other applications.

1. Introduction

Due to their use in many optoelectronic applications, semiconductor nanoparticles/polymer composites have drawn considerable attention in the latest years [1]. For example, a high concentration of TiO_2 nanoparticles in PVA matrix has a broad variety of CUT-OFF laser filters [2]. In the production of blue emitters, CdSe based polymer nanocomposites were used [3, 4]. The doped PVA matrix by silver nanoparticles showed improvements in their characteristics as elastic modulus and transition temperature compared to PVA alone [5].

One of the many polymers recognized today is polyvinyl alcohol (PVA). It has drawn significant attention as it is a water-soluble, biocompatible polymer material that is environmentally friendly [6–8]. Also, PVA has an excellent capacity for film-forming, excellent characteristics for adhesion and accepting metal nanoparticles nicely to exhibit magnetic characteristics.

Lead iodide, PbI_2 characterize by interesting photoconductive properties and optical applications. Because of the large bandgap (2.3–2.55 eV) and high atomic number ($\text{Pb} = 82$ and $\text{I} = 53$), PbI_2 could be used to detect x-ray and γ -ray radiations at room temperature with high efficiency [9]. PbI_2 has other properties like thermal stability and lower vapor pressure. Many physical characteristics become dependent on the size in a semiconductor nanoparticle.

In the present work, we have fabricated pure PVA film and PVA polymeric films doped with various quantities of PbI_2 nanoparticles using an ultrasonication homogenizer system [10] and casting techniques to disperse nanoparticles in polymeric matrices. Doping PbI_2 as nanocomposites in PVA can play an important role in modifying the PVA characteristics. Using x-ray diffraction, Fourier Transform Infrared Spectroscopy

(FT-IR) and scanning electron microscope (SEM), the structural characteristics of PbI₂/PVA nanocomposite films were studied. The optical and electrical characteristics of PbI₂/PVA nanocomposite films have been examined. Also, the samples optical limiting has been examined using He–Ne laser at 532 and 632.8 nm.

2. Experimental work

For the current work, all chemicals are purchased from Alfa Aesar and Sigma Aldrich: lead acetate [Pb(C₂H₃O₂)₂], sodium iodide (NaI), poly(vinyl alcohol) (PVA) and Cetyl trimethyl ammonium bromide (CTAB).

2.1. Synthesis of lead iodide nanoparticles (PbI₂ NPs)

For our PbI₂ synthesis, we used 1 M lead acetate (39.987 g) and 50 ml of dual- distilled water, 50 ml CTAB in one beaker step by step. Into another beaker, we dissolved 2 M sodium iodide (37.795 g) in 50 ml double distilled water. At room temperature, both solutions were dissolved evenly using a very stable 600 rpm magnetic stirrer. We mixed them very gently in the beaker after receiving the transparent solution and continually stirred then clear yellow solution was obtained which is identified as lead iodide (PbI₂). The hydrothermal method [11] has been reported to prepare pure PbI₂ solutions and nanostructures. The hydrothermal technique is regarded as the preferred method for preparing the nanoparticle semiconductor with well-controlling morphologies at reduced temperatures using a single-step process [12]. Lastly, the yellow solutions obtained washed attentively several times with dual distilled water and filtered and vacuum-dried for 24 h at 80 °C.

2.2. Samples preparation

A solution casting method was developed to produce PbI₂/PVA composite films. In 1 L of distilled water, nearly 22.5 g of PVA was dissolved for 24 h with a magnetic stirrer at 60 °C. Then, for about 120 min, the PVA solution acquired was cooled to room temperature to eliminate the bubbles. Separately, various content of PbI₂ nanoparticles varying from 0.14 wt% to 14.8 wt% was mixed with the above solution and the solution was subjected to ultrasonic treatment for 5 min at 110 watts. After that, the dispersed solution was stirred for 3 h. To acquire the nanocomposite films, the solution was then transferred into a Petri dish and dried in the air naturally. After that the samples were cut in suitable size for further investigations.

2.3. Characterizations of the nanocomposites

X-ray diffraction patterns are performed for PbI₂/PVA films using the Shimadzu LabX-XRD-6000 with CuK_α ($\lambda = 1.5406 \text{ \AA}$).

Fourier transformation Infrared Spectroscopy absorption spectra were recorded using spectrometer (FT-IR- Alpha II). For the studied samples, surface morphology was performed by using a scanning electron microscope (SEM), model (JSM- 6360) operated at 20 kV.

JASCO V-570 spectrometer was used to evaluate linear optical properties between 190 nm and 2500 nm at room temperature (the transmittance $T(\lambda)$ and absorbance $Abs(\lambda)$).

A programmable automatic LCR meter (Model FLUKE PM6306) for measuring the dielectric properties.

The optical limiting effect for PbI₂/PVA composite polymeric films was examined using two sources of He–Ne laser beam of wavelength equals 632.8 nm and the solid-state laser diode beam of wavelength equals 532 nm to get the normalized power of the nanocomposite films. The focal lens of the focal length of 10 cm was set on an optical bench on the front of the laser beam. Then, the sample holder was detached as the focal point of the lens. The input/output power was estimated by utilizing an optical measuring device connected to a photodetector (Model: Newport 1916-R).

3. Results and discussion

3.1. Structural behaviors of PbI₂-doped PVA nanocomposite films

3.1.1. XRD analysis of PbI₂-doped PVA nanocomposite films

The XRD technique was used to check the structural changes resulting from the addition of the PbI₂ nanoparticles in the PVA matrix. XRD patterns over a 2θ range of 10° to 70° have been detected. The 2θ of diffraction peaks of PbI₂ occur at 22.45, 25.94, 34.18, 38.56, 39.73, 41.72, 45.31, 47.85, 52.41, 53.28, 56.53, 61.61, 63.71, 67.65 and 68.44 as shown in figure 1(a). These peaks correspond to reflections of crystal plane (100), (011), (102), (003), (110), (111), (103), (200), (022), (113), (023), (114), (212) and (300), respectively. This reflects the hexagonal PbI₂ structure standard card (JCPDS:80-1000). Figure 1(b) shows the XRD pattern for PVA pure and PbI₂/PVA nanocomposite films. For pure PVA, one relatively sharp peak was observed at $2\theta = 19.11^\circ$ which are related to PVA's semi-crystalline nature [13, 14]. Yahia *et al* report a similar result [2]. The behavior PbI₂/PVA nanocomposites were the same as the pure PVA polymer, showing the same peaks, but it can be observed that

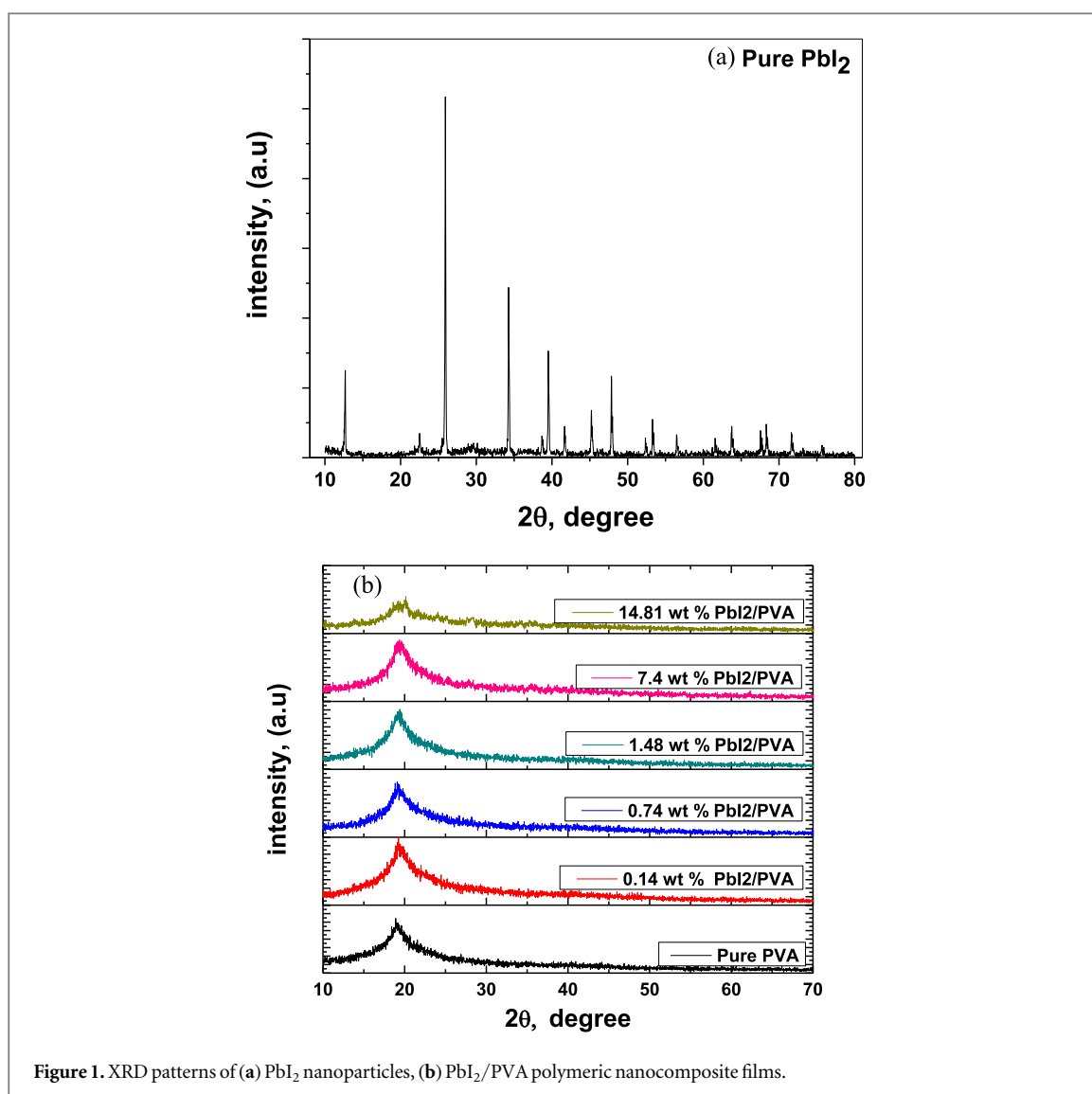


Figure 1. XRD patterns of (a) PbI₂ nanoparticles, (b) PbI₂/PVA polymeric nanocomposite films.

the addition of PbI₂ causes a shift of the $2\theta = 19.36^\circ$ with lower intensity and similar width between them. The sharp peaks of PbI₂ disappeared in PVA (figure 1(b)). When the PbI₂ nanoparticles were doping in the PVA matrix at a higher concentrations (14.81 wt%), the 2θ values increased (i.e. $2\theta = 20.16^\circ$) showing less intensity and the diffraction beak is broadening. This may be due to the electrons interaction [15] between PbI₂ and functional groups of the PVA causing disturbance of PVA hydrogen bonding [16]. This effect has been previously observed while doping TiO₂/PVA [2] and PbO₂/PVA [17].

The particle size P was evaluated based on the regular broadening of XRD peaks. This extension is a basic property of XRD outlined in Scherer's well-established theory [18, 19] and presented in table 1 as in the equation:

$$P = \frac{K\lambda}{\beta \cos \theta}, \quad (1)$$

where K is 0.9, λ is the wavelength ($=0.154$ nm), θ is the angle of deviation of the diffraction beam obtained from 2θ values corresponding to highest intensity peak in XRD pattern, and β is FWHM of the peak. Figures 2(a)–(f) showed that β can be obtained from observed FWHM of Gaussian fit. From figure 2 and table 1, the extended diffraction peak is associated directly with the lower particle size [20]. Table 1 shows that for pure PVA the average crystallite size is 3.45 nm and the average crystallite size value P reduces as dopant concentrations increase. The interplanar distance d was determined using Bragg's law [21]:

$$2d \sin \theta = n\lambda, \quad (2)$$

where d value equals 4.64 \AA , corresponding to (101) the plane of PVA's structure showing the semi-crystalline nature of the film and well matching the values reported [2]. The value of interplanar distance d also calculated and given in table 1. Apparently, the interplanar distance decreases slightly indicating an interaction between PVA and PbI₂ nanoparticles. This can be understood by estimating the average inter-crystallite separation in the

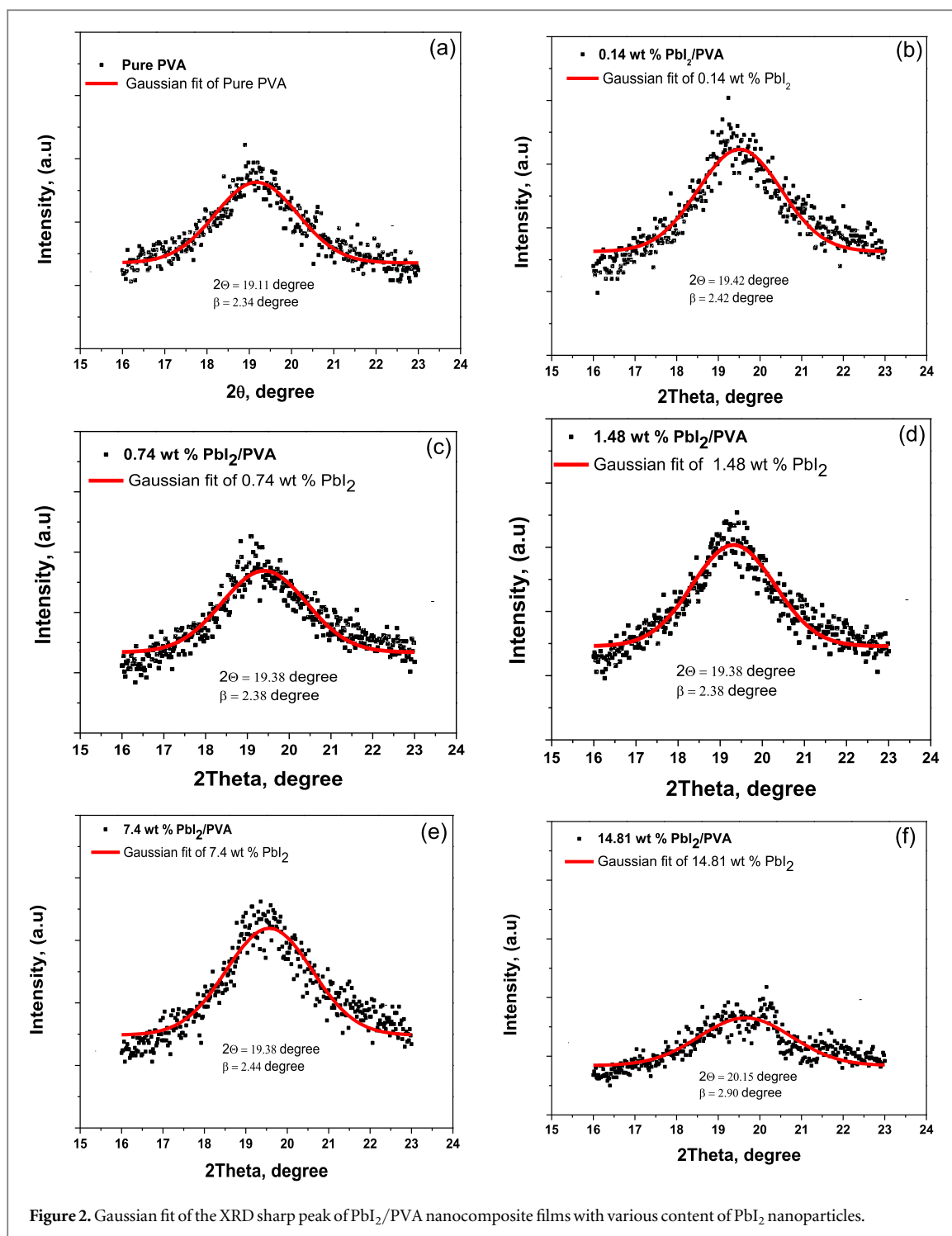


Figure 2. Gaussian fit of the XRD sharp peak of PbI_2/PVA nanocomposite films with various content of PbI_2 nanoparticles.

Table 1. Lattice parameters, d , R and P for PbI_2/PVA nanocomposite films.

Samples	P, Particle size, (nm)	d, spacing, Å	R, Average intercrystalline spacing, (nm)
PVA	3.45	4.64	0.578
0.14% wt of PbI_2/PVA	3.33	4.56	0.570
0.74% wt of PbI_2/PVA	3.17	4.58	0.573
1.48% wt of PbI_2/PVA	3.40	4.58	0.573
7.4% wt of PbI_2/PVA	3.30	4.58	0.573
14.81% wt of PbI_2/PVA	2.78	4.40	0.55

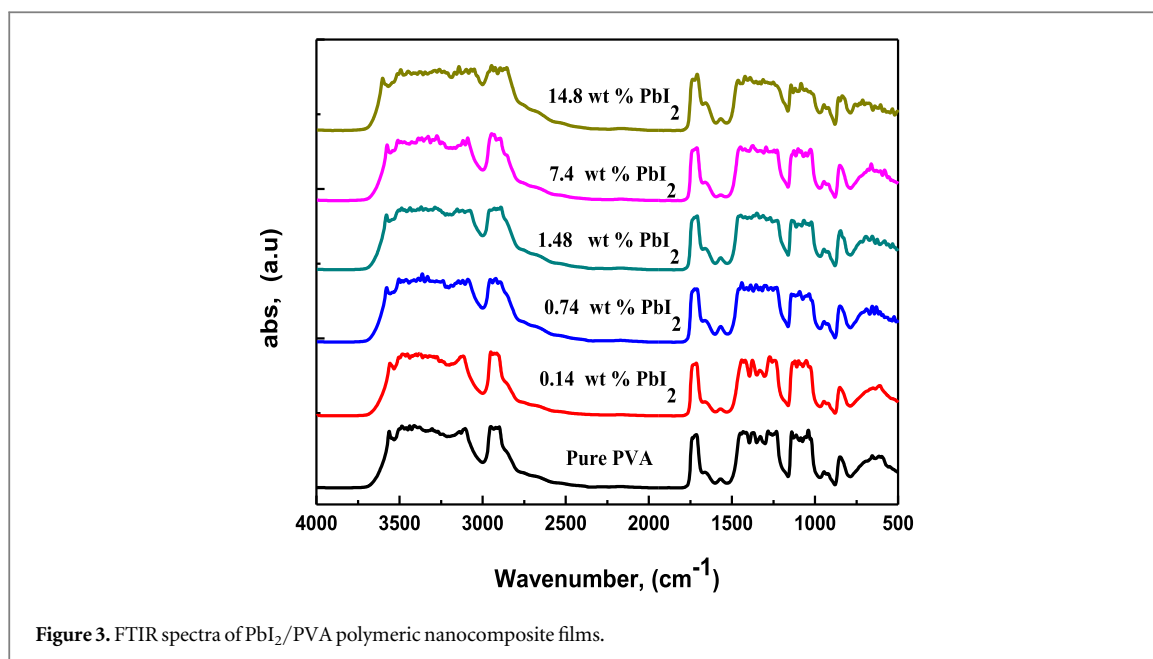


Figure 3. FTIR spectra of PbI₂/PVA polymeric nanocomposite films.

amorphous region R , that can be determined from the relation [22]:

$$R = \frac{5\lambda}{8 \sin \theta}, \quad (3)$$

Furthermore, table 1 tabulated the average inter-crystallite separation in the amorphous region R . For pure PVA, the R -value is 0.578, which decreases with the higher PbI₂ concentration indicating interaction of Pb⁺² with the hydroxyl (OH) groups and the carbonyl group (>C=O) of the PVA polymeric chain. This result obtained in previous work with MnCl₂/PVA [23].

3.1.2. Fourier transform infrared spectroscopy (FT-IR) of PbI₂-doped PVA nanocomposite films

In the range of wavenumber between 400 cm⁻¹ to 4000 cm⁻¹, an analysis of the FT-IR was carried out to estimate the ability of PbI₂ nanoparticles to interact with the polymeric PVA matrix. Figure 3 indicates the FT-IR spectra obtained for pure PVA and for each of its PbI₂ nanocomposites. FT-IR shows the characteristic of functional groups of PVA polymer [24]. Pure PVA exhibited strong broad peak in-band range 3503–3105 cm⁻¹ because of (O–H) stretch vibrations and another peak at 2951–2900 cm⁻¹ given (CH₂) asymmetric stretching. The peak observed at 1738 cm⁻¹ could be allocated to carbonyl (C=O) stretching bond, while 1040 cm⁻¹ indicated (C–O) stretching presence. A weak band at 849 cm⁻¹ pointed to (C–C) stretching. At low concentration of PbI₂, small shifting in peaks can be observed. Increasing the PbI₂ concentration causing the shift of (O–H) stretching vibrations to range 3601–3050 cm⁻¹ and shifting (CH₂) asymmetric stretching to 2946–2854 cm⁻¹. Also, the carbonyl stretching bond shifted to 1735 cm⁻¹ while (C–O) stretching assigning to 1054 cm⁻¹. These results may support the chemical interaction between nanoparticles and polymer matrix. New absorption bands at ~713 cm⁻¹ [25] were appeared, which indicated the formation of a new chemical bond in the PbI₂/PVA nanocomposites. This result suggested that the structure of PVA altered by the interactions with PbI₂ as a result of some additional peaks and shifts in frequencies when compared with pure PVA.

3.1.3. Scanning electron microscope (SEM) of PbI₂ doped PVA nanocomposite films:

SEM presents the morphology and structure of nanomaterials. Figure 4 showed the SEM images for the PVA including different weight percentages of PbI₂. From figure 4(a), it is evident a clear and smooth surface area of pure PVA which demonstrates PVA transparency. Figures 4(b)–(d) displayed PbI₂/PVA nanocomposite samples with different wt% ratios of PbI₂ in PVA matrix. It was possible to see that, the PbI₂ nanoparticles were dispersed homogeneously in the PVA matrix. As the PbI₂ concentration increases, the size of PbI₂ particles increases, and agglomerating the PbI₂ nanoparticles. This phenomenon shows that high concentrations of PbI₂ can influence PbI₂ agglomeration. The surface area is reduced as the particle size rises and the contact between the particles rises this also increases the conductivity of PbI₂/PVA nanocomposites.

3.2. Optical analysis of PbI₂ doped PVA nanocomposite films

Figure 5 presents the transmission spectra in the wavelength range (200–2500 nm) of pure PVA and its different PbI₂ concentrations in PVA polymer matrix. The transmittance increases in the range 200 to 375 nm, then

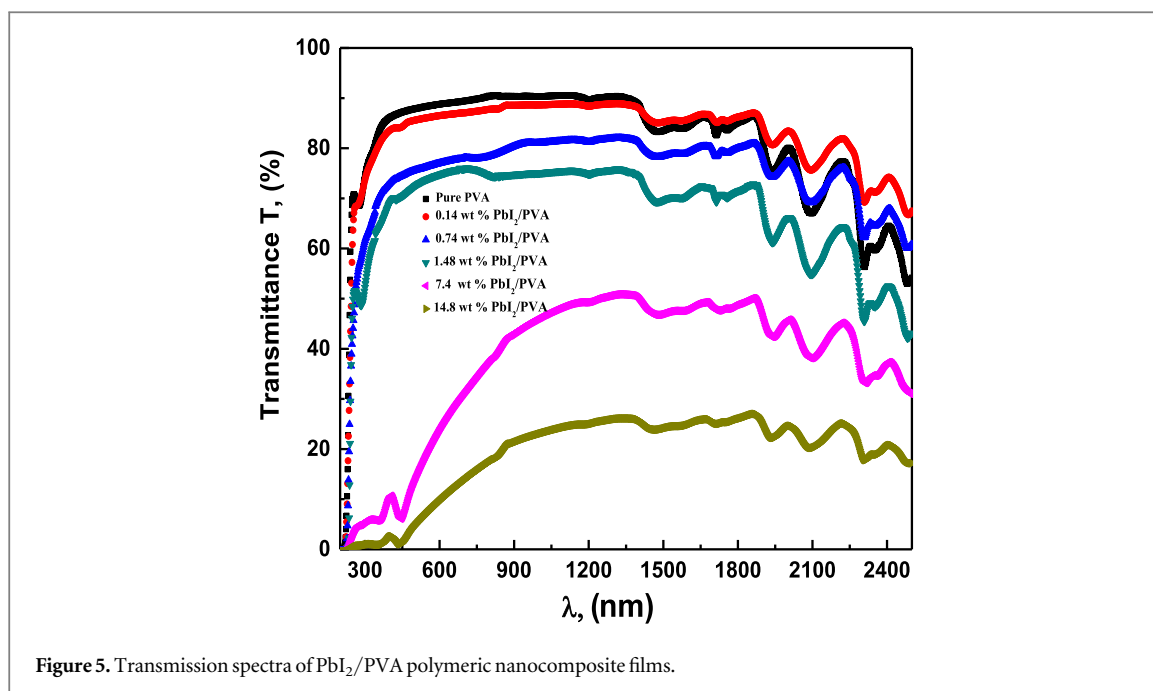


Figure 5. Transmission spectra of PbI_2/PVA polymeric nanocomposite films.

3.2.1. Determination of the optical bandgap of PbI_2/PVA nanocomposites films

Urbach's relation describes the absorption coefficient closing to the absorption edge [30, 31] bandgap which provides helpful data on the level of defects in the optical material scheme. The Urbach's energy (E_U) can be calculated using the relationship below [30]:

$$\alpha = \alpha_0 e^{hv/E_U}, \quad (4)$$

where α_0 is a constant. Figure 7 shows the variation between $\log \alpha$ and hv of pure PVA and PbI_2/PVA films. The variation in α was low at low frequencies and increased at the greater frequencies. This may be due to the interband transition at high photon energy [26]. The E_u values are computed from the slope's reverse. Table 2 presents the Urbach's energy values for pure PVA and nanocomposite films. It is evident from table 2 that E_U values are raising with PbI_2 nanoparticles in PVA polymeric matrix, this may be attributed to the creation of localized states due to PbI_2 doping. Yahia *et al* reported this behavior before while doping TiO_2/PVA [2] nanocomposites (see table 2).

An essential tool for determining bandgap is the optical absorption spectrum which can be explained the electronic band structure of semiconductors. The optical band gap is the lowest energy transition between the HOMO and LUMO states. The optical bandgap energy (E_g) is the absorption resulting from transitions between valence and conductive band states located closed to the respective mobility edges. The following equation predicted the optical band gap energy [32, 33]:

$$\alpha hv = B (hv - E_g)^m, \quad (5)$$

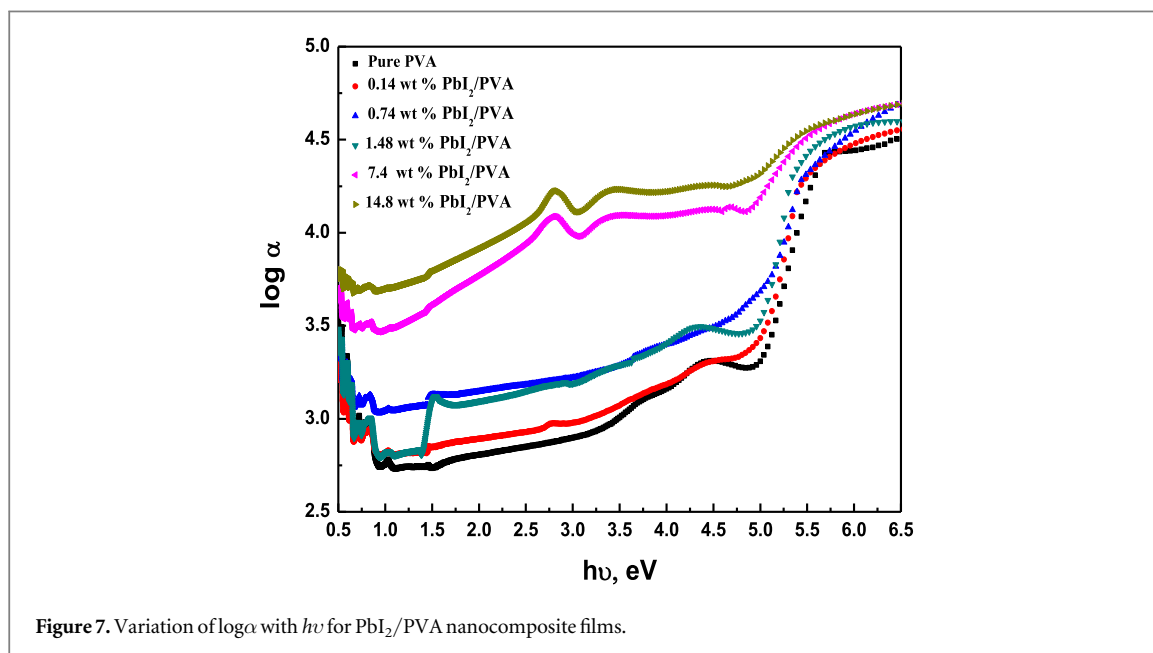
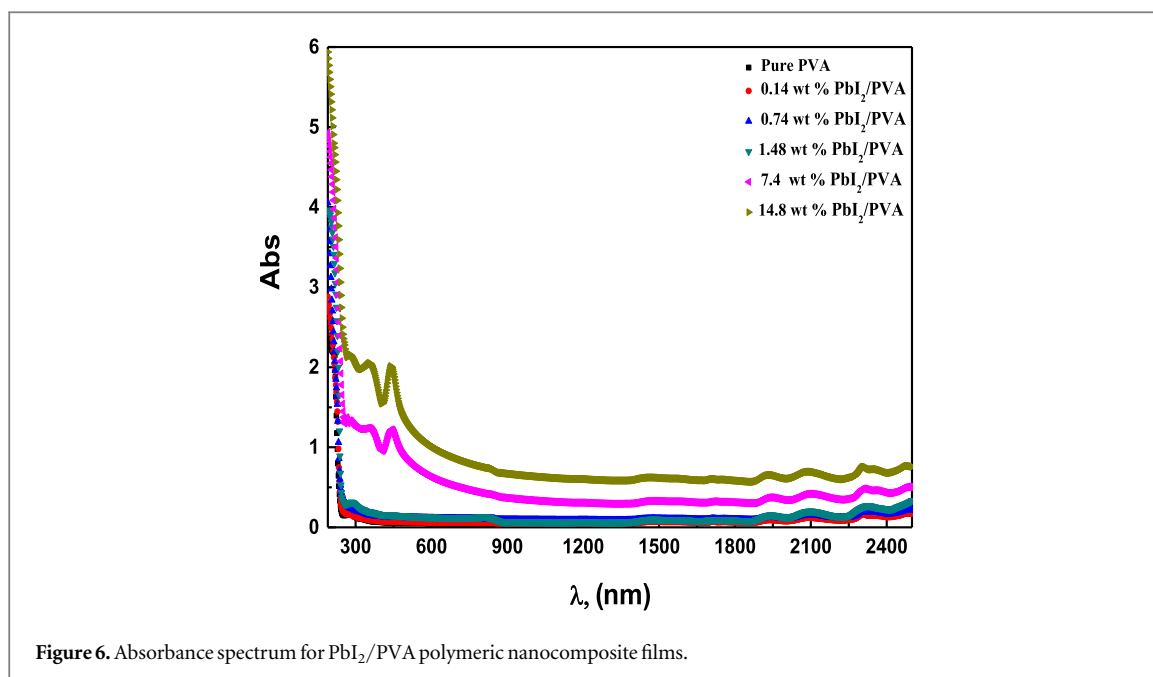
where α is the absorption coefficient, hv is the photon energy and B is a variable dependent on transition probability which could be assumed to be constant within the range of the optical frequency, m is used to define the electronic transitional form and is associated with state density distribution. The m requires 1/2 to transition directly and 2 to transition indirect [32–34]. PVA can have both direct and indirect band gaps. In order to achieve an indirect bandgap, $(\alpha hv)^{1/2}$ was plotted against photon energy (hv) for pure PVA and the PbI_2 nanocomposite system as shown in figure 8, then extrapolate the linear part of the curve to $(\alpha hv)^{1/2} = 0$. The indirect bandgap for pure PVA is 5.00 eV and that for the studied nanocomposite system of the PbI_2/PVA films is 4.91–3.49 eV.

Similarly, the plot of $(\alpha hv)^2$ against hv had been used for obtaining the direct bandgap energy for pure PVA and the PbI_2 polymeric nanocomposite system as shown in figure 9. The direct bandgap energy for pure PVA is 5.48 eV and 5.28–4.88 eV for PbI_2/PVA polymeric nanocomposite films obtained from the linear curve extrapolation to a point $(\alpha hv)^2 = 0$. The calculated values for indirect and direct bandgap energy are presented in table 2. The decrease by raising the doping concentration in the values of indirect and direct bandgap energy may lead to the creation of localized states in E_g owing to PbI_2 doping. This behavior has been reported before in ZnI_2/PVA [27], GO/PVA [26] and TiO_2/PVA [2, 28] nanocomposites (see table 2). Also, the indirect energy band gap is smaller than the direct energy bandgap in all concentrations [26].

It is possible to calculate the extinction index, k associated with the wavelength, λ , and the absorption coefficient, α using the following expression:

Table 2. The Transmittance, E_U , indirect and direct energy band gap, and n for PbI_2 /PVA polymeric nanocomposite films.

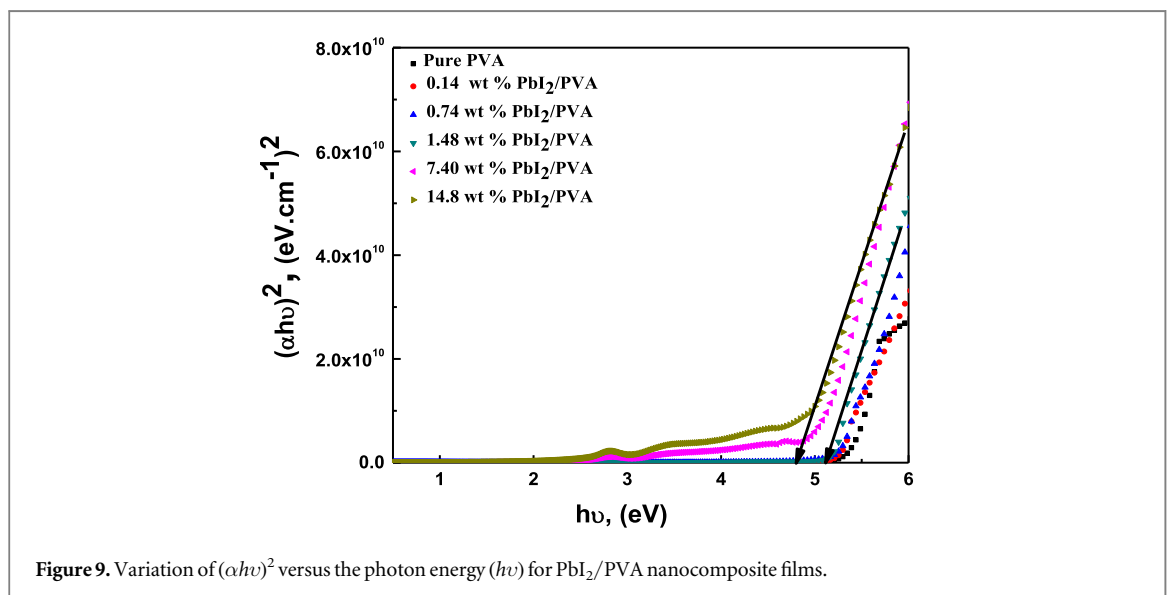
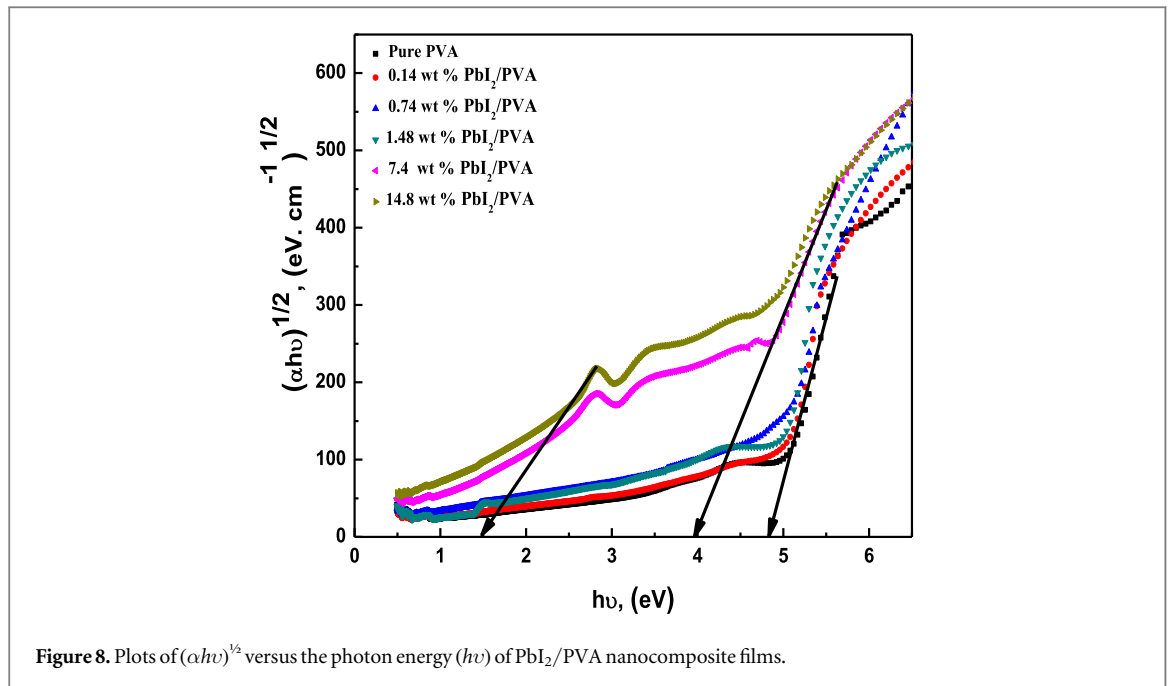
Samples	T_{max} 450 nm	T_{max} 1200 nm	E_U	E_g indirect eV		E_g direct eV	n	
				E_{g1}	E_{g2}			
Pure PVA	87.05	89.48	0.51	5.00	—	5.48	1.21	Present work
0.14 wt% of PbI_2 /PVA	84.09	88.42	0.57	4.91	—	5.28	1.32	
0.74 wt% of PbI_2 /PVA	74.26	81.27	0.65	4.88	—	5.38	1.35	
1.48 wt% of PbI_2 /PVA	70.61	75.16	0.36	4.80	—	5.19	1.38	
7.4 wt% of PbI_2 /PVA	6.37	50.47	1.44	4.06	1.5	5.01	1.46	
14.81 wt% of PbI_2 /PVA	1.80	25.00	1.91	3.49	1.44	4.88	1.42	
ZnI ₂ /PVA 1.85 wt%-37.03wt%	85–10	85–75	—	4.733–4.171	3.293–2.864	—	—	[27]
GO/PVA 0.37 wt%- 9.259 wt%	87–25	90–40	—	4.55-0.95	—	5.92–5.4	—	[26]
TiO ₂ /PVA 0.037 wt%-37.037 wt%	~80–0	~80–4	0.31–15.9	—	—	5.6–1.82	1.255–2.06	[2]
TiO ₂ /PVA 1.3 wt%-6.6 wt%	—	—	—	—	—	3.87–2.79	—	[28]
PbO ₂ /PVA 0.05 M- 0.2 M	—	—	—	—	—	6.32–4.33	1.15–1.42	[17]



$$k = \alpha \lambda / 4\pi, \quad (6)$$

Figure 10 illustrates the variance of k versus λ for the PVA and the different PbI₂/PVA nanocomposite films. From figure 10, it is noticed that as photon energy increases, the extinction coefficient first reduces and then increases from 300 nm to 1800 nm for all the samples.

The refractive index (n) is another basic physical parameter when developing new optical device material assigning the material optical systems and electronic features. High refractive index optical materials are recommended in different fields [34, 35]. Figure 11 illustrates the change of n with λ of light for pristine PVA film and different nanocomposite films. For pure PVA, the refractive index sharply decreases with increasing the wavelength till 300 nm then decreases slowly. The refractive index n is strongly associated with electronic ion polarization and the local fields within materials which rises with frequency [36] so, the n value also increases with frequency and decreases with wavelength. Table 2 shows the refractive index for pristine PVA and various nanocomposite films at 600 nm wavelength. The n values increase by increasing the doping concentration as shown in table 2. Such a refractive index rise is comparable to that discovered in the nanocomposite system with TiO₂/PVA by Yahia *et al* [2] and PbO₂/PVA by Rebar T Abdulwahid *et al* [17]. This increasing in n value may be due to the interaction of PbI₂ nanoparticles with the PVA matrices.



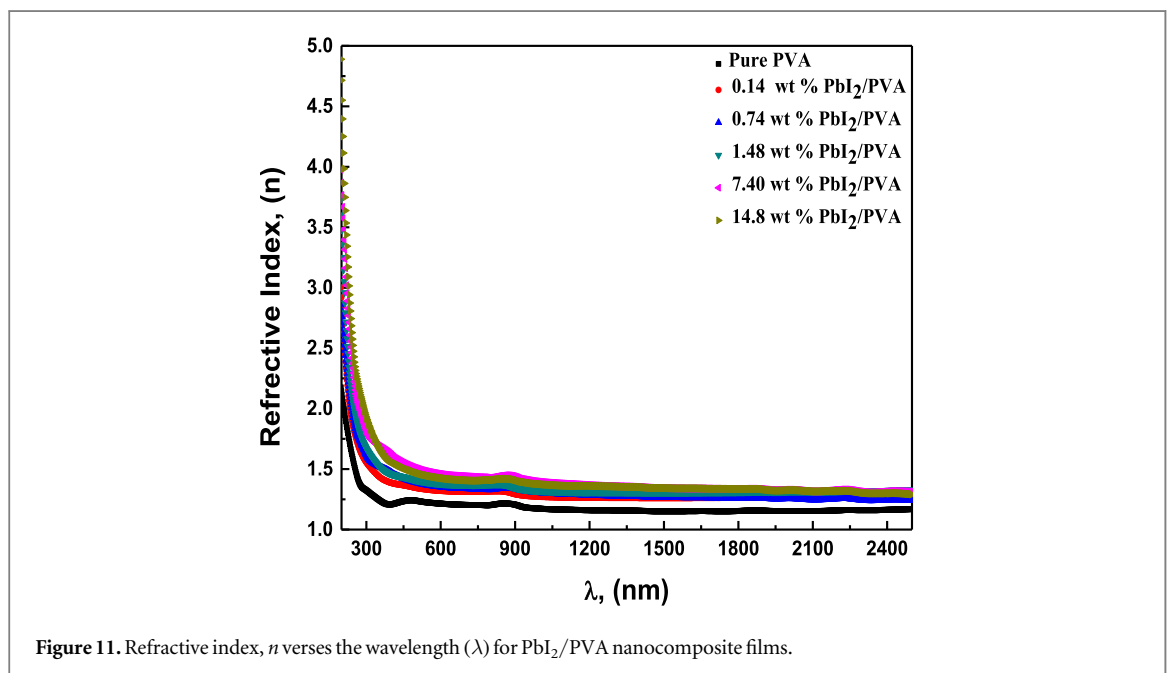
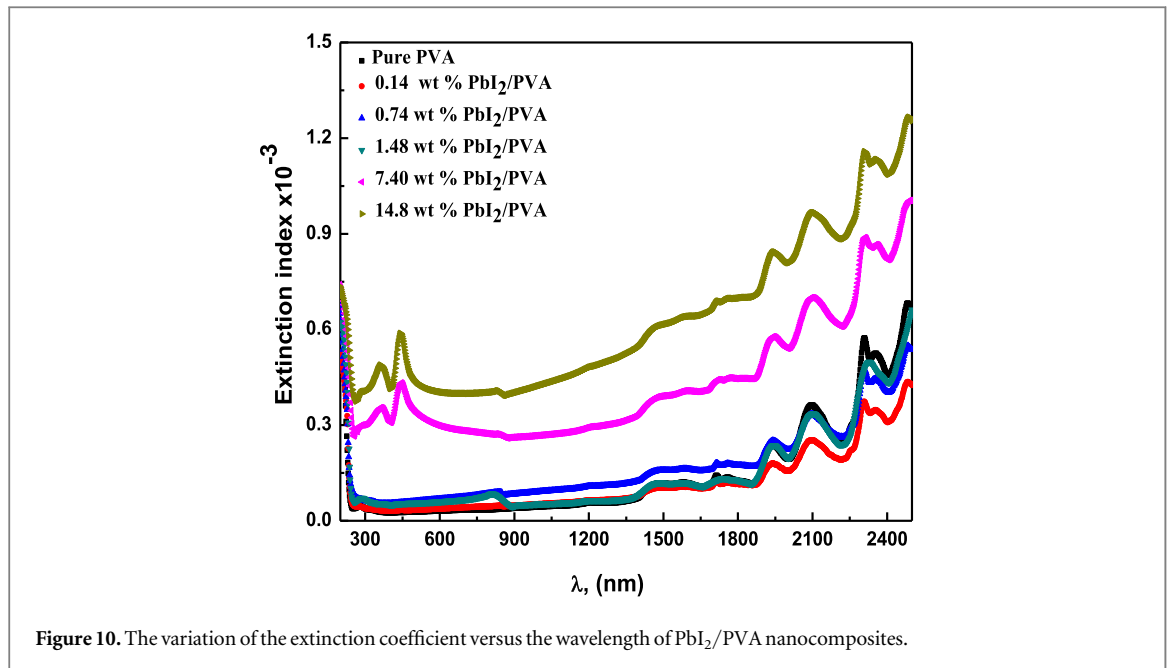
The optical conductivity, σ is a useful tool for studying the electronic states in materials. Optical conductivity is linked to the refractive index n and the absorption coefficient α by the equation: $\sigma = \frac{\alpha n c}{4\pi}$, where c is the light velocity [34, 37]. Figure 12 shows the optical conductivity of pure PVA and PVA/ PbI_2 nanocomposite films. It is noted that σ values increase with increasing frequency. Also, the conductivity values orderly increase with increasing PbI_2 content, which is more sensible at a lower frequency. This increase in conductivity means that the bandgap decreases because new levels are created in it. So, the optical conductivity σ can be controlled by the PbI_2 doping percentage.

3.3. Dielectric properties of PbI_2/PVA nanocomposites films

Dielectric measurements in polymeric materials are a powerful technique for obtaining information on mechanisms of conduction and relaxation. The dielectric constant ϵ_1 and dielectric loss values ϵ_2 have been computed based on the following equations:

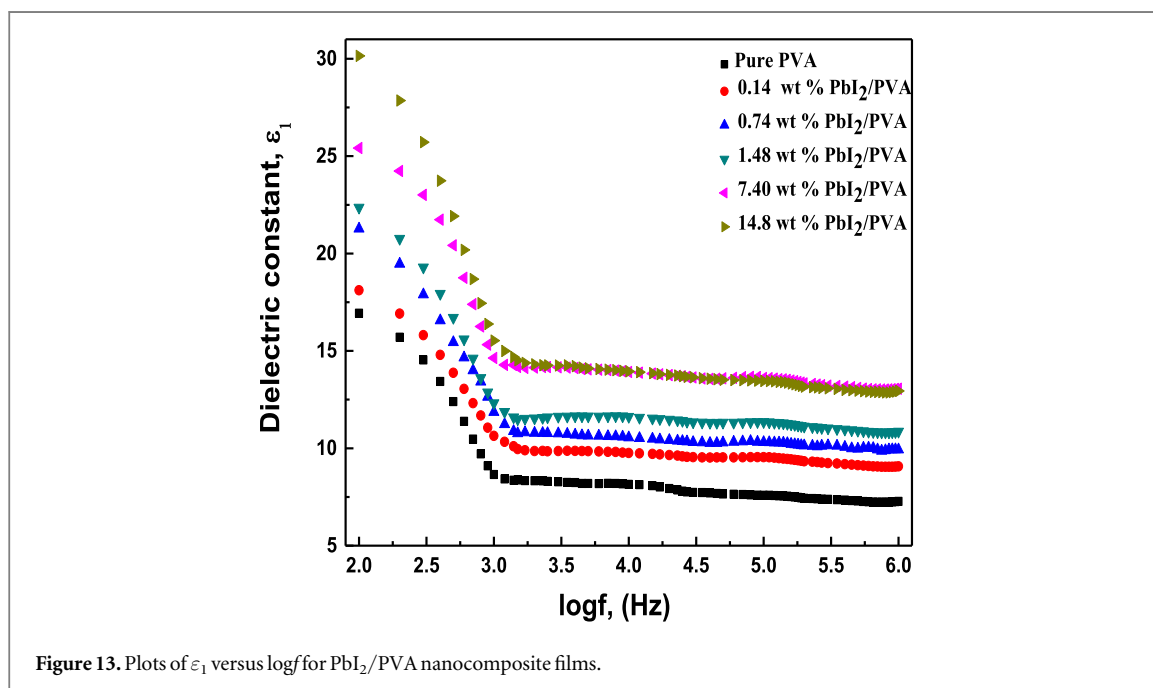
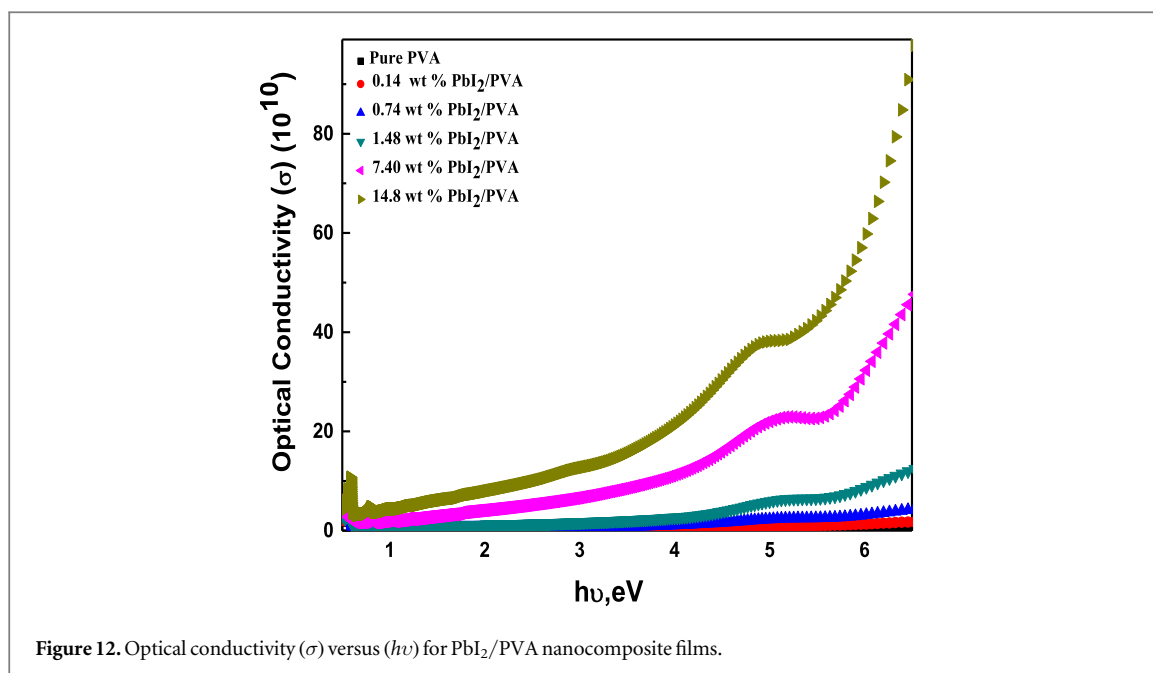
$$\epsilon_1 = \frac{C t}{\epsilon_0 A} \text{ and } \epsilon_2 = \epsilon_1 \tan \delta, \quad (7)$$

It can be seen from figures 13 and 14, the change of ϵ_1 and ϵ_2 with frequency respectively. The obtained values of ϵ_1 and ϵ_2 of pure PVA and different nanocomposites, PVA/ PbI_2 at 100 Hz are tabulated in table 3. At lower



frequency, the dielectric constant performs the highest value then reduces as frequency increases as shown in figure 13. This can be linked to the tendency to be oriented towards the field applied at the low-frequency range of dipoles in polymeric films while at high-frequency dipoles have smaller tendency to be oriented according to the field variations due to polarization effects. Thus, the dielectric constant value reduces [38]. It is also clearly observable from figure 13 that the dielectric constant increases for higher concentration of dopant PbI₂ nanoparticles perform lowest value for pure PVA (see table 3).

From figure 14, dielectric loss decreases with increasing frequency. The greater value of low-frequency dielectric loss may be caused by the mobile charges in the polymeric matrices. At low frequency, the values of ϵ_2 increase with increasing PbI₂ concentrations (see table 3), the dielectric loss increase may be due to the dipole charge increase. While, at high frequency, the change in dielectric loss with frequency and concentration is very low because the regular field inversion is so rapid in the direction of the electric field so there is no surplus ion diffusion [39, 40]. This result could be described based on electrical conductivity σ_{ac} that is related to ϵ_2 . To investigate the effect of doping PbI₂ nanoparticles on the AC electrical conductivity σ_{AC} of PVA polymeric films, calculations were performed using the following equation:



$$\sigma_{AC} = \omega \epsilon_0 \epsilon_1 \tan \delta = 2\pi f \epsilon_0 \epsilon_2, \quad (8)$$

where ω is the angular frequency ($=2\pi f$), f is the applied frequency, ϵ_0 is the permittivity of the free space, $\tan \delta = \epsilon_2 / \epsilon_1$ and ϵ_2 represents the dielectric loss. Figure 15 illustrates the variability of σ_{AC} for pure PVA and PbI₂/PVA nanocomposite films with frequency. As the frequency rises, σ_{ac} increases as shown in figure 15. Also, AC electrical conductivity improves with increasing dopant concentration. In general, the frequency dependency of $\sigma_{AC}(\omega)$ follows the universal power law:

$$\sigma_{AC} = A \omega^s, \quad (9)$$

where A and s are constants of the material. It is possible to calculate the exponent (s) from $\ln \sigma_{AC}$ plots against $\ln \omega$. Figure 16 represents the variation of the frequency exponent s with PbI₂ content. From figure 16, it can be noticed that the s value decreases by increasing the PbI₂ concentration which means that the higher concentration increase, AC electrical conductivity increases. This result supports the conduction by the correlated barrier hopping (CBH) model. This result obtained in previous work with GO/PVA [26].

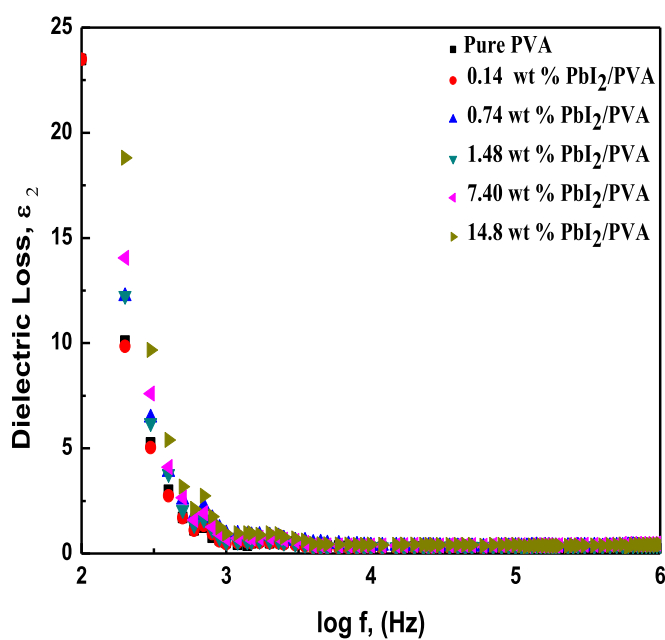


Figure 14. Plots of ϵ_2 versus $\log f$ for PbI_2/PVA nanocomposite films.

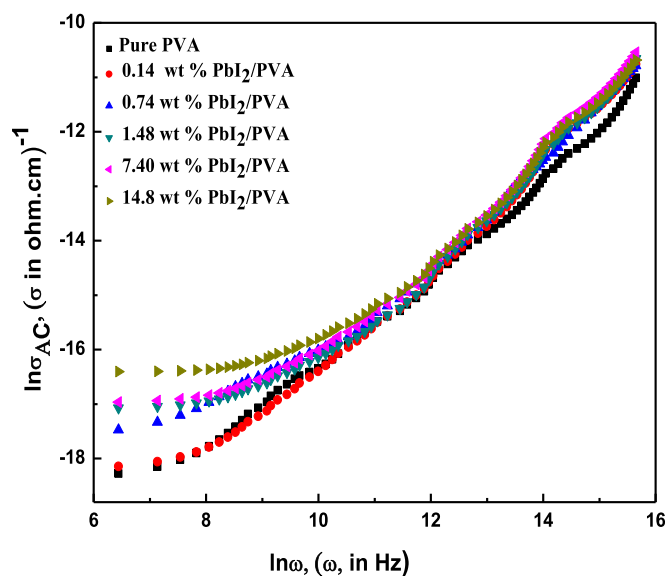
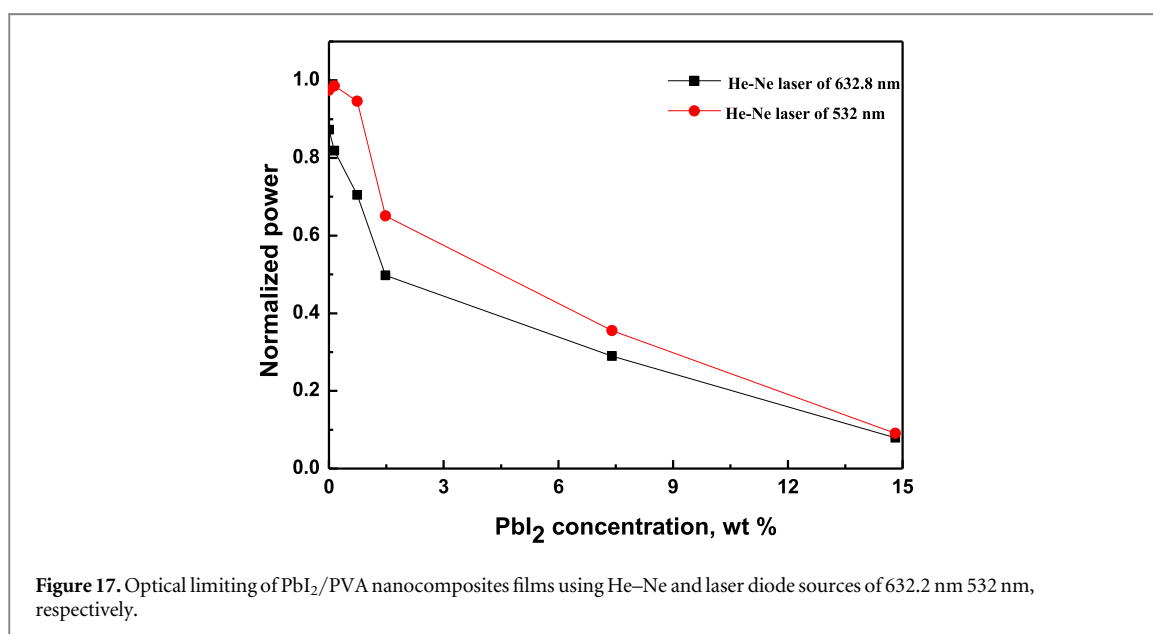
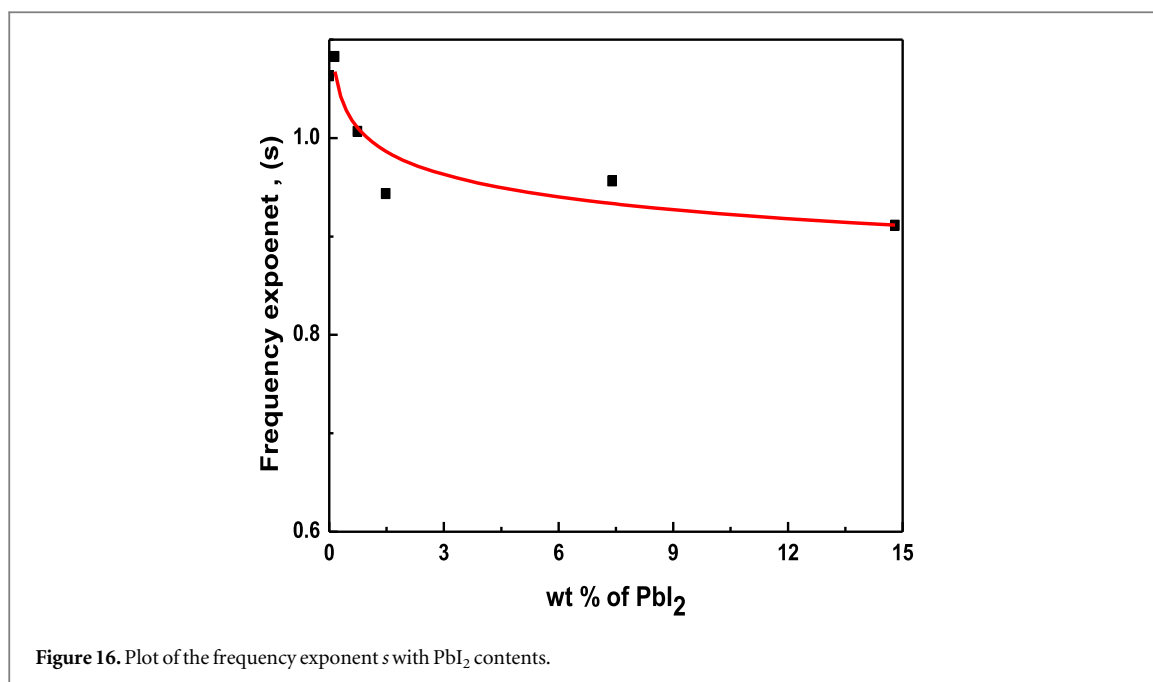


Figure 15. AC electrical conductivity σ_{AC} with frequency for PbI_2/PVA nanocomposite films.

Table 3. The dielectric constant and dielectric loss for PbI_2/PVA polymeric nanocomposite films.

Samples	ϵ_1	ϵ_2
Pure PVA	16.93	23.48
0.14 wt% of PbI_2/PVA	18.12	23.49
0.74 wt% of PbI_2/PVA	21.27	27.31
1.48 wt% of PbI_2/PVA	22.36	30.60
7.4 wt% of PbI_2/PVA	25.42	36.17
14.81 wt% of PbI_2/PVA	30.15	44.65



3.4. The optical limiting of PbI₂/PVA nanocomposites films

An optical limitation is an effect that keeps the power, irradiance, energy, or fluence that an optical system transmits below the maximum value, regardless of the magnitude of the input [41]. It must do this while maintaining high transmittance at low input powers. Studies of optical power limitation of PbI₂/PVA nanocomposites were examined using He-Ne laser at 632.8 nm and the solid-state laser diode beam at 532 nm [42, 43]. Figure 17 explains the variation of the optical output power with PbI₂ weight percent. The source's main power is 5×10^{-4} W. With increasing concentration of PbI₂ the normalized power is decreased which indicates the good optical limiting behavior. It could be noticed that the normalized power decrease with increasing laser power intensity for all samples. The most expanded applications of such an effect are the protection of sensitive optical sensors and components from laser damage and applications in nonlinear optical devices.

4. Conclusion

PVA and PbI₂/PVA nanocomposite films were developed by ultrasonication and solution casting methods. The sample's structural information carried by XRD, FT-IR, and SEM which reveal that the structure of PVA altered

by the interactions with PbI_2 especially at 7.4 wt% and 14.8 wt% when compared with pure PVA. The optical studies investigate that the transmission reduces and the absorption edge shifts to longer wavelengths by increasing the content of PbI_2 nanoparticles in PVA (7.4 wt% and 14.8 wt%) which could be assigned to the presence of lead iodide additive in the PVA matrix and the production of some aggregates of PbI_2 nanoparticles within the polymeric matrix. Also, the addition of PbI_2 into the PVA matrix can increase Urbach's energy and reduce the optical band gap energy, directly and indirectly give a better photoconductive response. So, this film's bandgap can play an essential role in optoelectronic devices.

The dielectric constant and dielectric loss reduce with increasing frequency. The dielectric constant increases with increasing concentration which is less sensitive for dielectric loss. AC electrical conductivity rises with frequency and PbI_2 dopant levels that promote the correlated barrier hopping (CBH) model for the conduction mechanism.

Using the He-Ne power laser beam $\sim 376 \mu\text{W}$ and $\lambda = 632.8 \text{ nm}$ and the solid-state laser diode beam of power $\sim 15.96 \text{ mW}$ and $\lambda = 532 \text{ nm}$ to study the attenuation capabilities of the studied nanocomposite films shows that the normalized power decrease with increasing laser power intensity for all samples.

So, the PbI_2/PVA nanocomposite dielectrics behave as good optical limiters. The results show that the nanostructures prepared are widely applied in the field of optoelectronics, radiation detection, and several other applications.

Acknowledgments

The authors are grateful to The Research Center for Advanced Material Science (RCAMS) at King Khalid University, with grant number (RCAMS-KKU/001-19).

ORCID iDs

M I Mohammed  <https://orcid.org/0000-0001-9402-8140>

I S Yahia  <https://orcid.org/0000-0002-9855-5033>

References

- [1] Bala V, Tripathi S K and Kumar R 2014 *Mater. Lett.* **132** 38–40
- [2] Yahia I S, Mohammed M I and Nawar A M 2018 *Multifunction, Physica B: Physics of Condensed Matter* **556** 48–60
- [3] Sooklal K, Hanus L H, Ploehn H J and Murphy C J 1998 A blue emitting CdS/dendrimer nanocomposite *Adv. Mater.* **10** 1083–7
- [4] Mbhele Z, Salemane M, Van Sittert C, Nedeljkovic J, Djokovic V and Luyt A 2003 *Chem. Mater.* **15** 5019–24
- [5] Pattabi M, Amma B S and Manzoor K 2007 *Mater. Res. Bull.* **42** 828–35
- [6] Ghanipour M and Dorrnian D 2013 *J. Nanomater.* **2013** 897043
- [7] El-Kader F H A, Hakeem N A, Elashmawi I S and Ismail A M 2013 *Aust. J. Basic Appl. Sci.* **7** 608–19
- [8] Tunc T, Altindal S, Dokme I and Uslu H 2011 *J. Electron. Mater.* **40** 157–64
- [9] Condeles J F, Ando R A and Mulato M 2008 *J. Mater. Sci.* **43** 525–9
- [10] Kaboorani A., Riedl B and Blanchet P 2013 *J. Nanomater.* **2013** 341897
- [11] Shkir M, Yahia I S, AlFaify S, Abutalib M M and Muhammad S 2016 *J. Mol. Struct.* **1110** 83–90
- [12] Schiebera M, Zamoshchik N, Khakhana O and Zucka A 2008 *J. Cryst. Growth* **310** 3168–73
- [13] Sarma S and Datta P 2010 *Nanosci. Nanotechnol. Lett.* **2** 261–5
- [14] Shujahadeen B A Z I Z 2016 *J. Electron. Mater.* **45** 736–45
- [15] Abdullah O, Aziz S B, Omer K M and Salih Y M 2015 *J. Mater. Sci., Mater. Electron.* **26** 5303–9
- [16] Chahal R P, Mahendia S, Tomar A K and Kumar S 2012 *J. Alloys Compd.* **538** 212–9
- [17] Abdulwahid R T, Abdullah O G, Aziz S B, Hussein S A, Muhammad F F and Yahya M Y 2016 *J. Mater. Sci., Mater. Electron.* **27** 12112–8
- [18] Alexander L and Klug H A 1950 Determination of crystallite size with the x-ray spectrometer *J. Appl. Phys.* **21** 137–42
- [19] Molefe F V, Koao L F, Dejene B F and Swart H C 2015 *Opt. Mater.* **46** 292–8
- [20] Aziz S B, Abdulwahid R T, Rsaul H A and Ahmed H M 2016 *J. Mater. Sci., Mater. Electron.* **27** 4163–71
- [21] Yahia I S, Bouzidi A, Zahran H Y, Jilani W, AlFaify S, Algarni H and Guermazi H 2018 *Journal of Molecular Structure* **1156** 492–500
- [22] Praveena S D, Ravindrachary V, Bhajantri R F and Ismayil 2016 *Polym. Compos.* **37** 987–97
- [23] Banerjee M, Jain A and Mukherjee G S 2019 *Polymer Composites* **40** E765–75
- [24] Liu Y, Ren W, Zheng L Y and Yao X 1999 *Thin Solid Films* **353** 124
- [25] Kaviyarasu K, Sajan D, Selvakumar M S, Augustine Thomas S and Prem Anand D 2012 *a, n Journal Of Physics And Chemistrt For Solids* **73** 1396–400
- [26] Yahia I S and Mohammed M I 2018 *J. Mater. Sci., Mater. Electron.*
- [27] Bouzidi A, Jilani W, Guermazi H, Yahia I S, Zahran H Y and Sakr G B 2019 *Journal of Materials Science, Materials in Electronics*
- [28] El-desoky M M, Morad I M, Wasfy M H and Mansour A F 2017 *IOSR Journal of Applied Physics* **9** 33–43 Ver. III
- [29] Furniss B S, Hannaford A J, Smith P W G and Tatchell A R 1991 *Vogel's Text Book of Practical Organic Chemistry* 5th ed (New York, NY: Wiley)
- [30] Urbach F 1953 *Phys. Rev.* **92** 1324
- [31] Studenyak I, Kranjcec M and Kurik M 2014 *Int. J. Opt. Appl.* **4** 76
- [32] Mott N F and Devis N F 1979 *Electronic Process in Noncrystalline Materials* 2nd ed (Oxford: Oxford University Press) p 273
- [33] Tauc J 1972 *Optical Properties of Solid* ed F Abeles (Amsterdam: North-Holland) pp 277–313

- [34] Abdullah O G, Aziz S B, Omer K M and Salih Y M 2015 *J. Mater. Sci. Mater.* **26** 5303
- [35] Ayedta I, Illarramendi M A, Arrue J, Parola I, Jiménez F, Zubia J and Koike Y 2017 *Polymers* **9** 90
- [36] Goswami A 2003 *Thin Film Fundamentals, New Age International* (New Delhi: Publishers)
- [37] Wongpaibool V 2018 Optical fibre characteristics and system configurations *VirginiaTech, Dissertation, Improvement of fiber optic system permormance by Synchronous phase Modulation and filtering at the Transmitter*. https://thesis.lib.vt.edu/theses/available/etd-02042003-164941/.../02_Ch2.pdf
- [38] Ramya C S, Savutha T, Selvasekarapandian S and Hirankumar G 2005 *Ionics* **11** 436–41
- [39] Bhargav P B, Sarada B A, Sharma A K, Rao V V R N and Macromol J 2010 *Sci. Part A:Pure Appl. Chem.* **47** 131–7
- [40] Mardare D and Rusu G I 2004 *J. Optoelectron. Adv. Mater.* **6** 333–6
- [41] Rashidian M and Dorrnian D 2015 Investigation of optical limiting in nanometals *Rev. Adv. Mater. Sci.* **40** 110–26
- [42] Liu Z, Zhang X, Yan X, Chen Y and Tian J 2012 *Chin. Sci. Bull.* **57** 2971–82
- [43] Tamgadge Y S, Sunatkari A L, Talwatkar S S, Paturkar V G and Muley G G 2016 *Opt. Mater.* **51** 175–84